Journal of Fluids and Structures 17 (2003) 415–431

JOURNAL OF FLUIDS AND STRUCTURES

www.elsevier.nl/locate/jnlabr/yjfls

Nonlinear statics and dynamics of a simply supported nonuniform tube conveying an incompressible inviscid fluid

S.V. Sorokin*, A.V. Terentiev

Department of Engineering Mechanics, State Marine Technical University of St. Petersburg, Lotsmanskaya Str.3, St.Petersburg, 190008, Russia

Received 6 March 2001; accepted 17 May 2002

Abstract

Nonlinear static and dynamic behaviour of a simply supported fluid-conveying tube, which has a constant inner diameter and a variable thickness is analysed analytically and numerically. Nonlinear static bending is considered in two loading cases: (i) a tube subjected to supercritical axial compressive forces acting at its edges or (ii) a tube loaded by concentrated bending moments, which provide a symmetrical (with respect to the mid-span) shape of a tube. The nonlinear governing equations of motions are derived by using Hamilton's principle. The elementary plug flow theory of an incompressible inviscid fluid is adopted for modelling a fluid–structure interaction. The flow velocity is taken as the sum of a principal constant 'mean' velocity component and a fairly small pulsating component. Firstly, eigenfrequencies and eigenmodes of a deformed tube are found from linearised equations of motions. Then resonant nonlinear oscillations of a tube about its deformed static equilibrium position in a plane of static bending are considered. A multiple scales method is used and a weak resonant excitation by the flow pulsation is considered in a single-mode regime and in a bi-modal regime (in the case of an internal parametric resonance) and the stability of each of them is examined. The brief parametric study of these regimes of motions is carried out.

1. Introduction

Flexible fluid-conveying tubes are widely used in various applications, e.g., fuel supply systems, chemical industry, medical equipment, etc., for connections between various vessels and appliances. These tubes are often exposed to dynamic loading, including flow pulsation. Then it is of a practical relevance to check whether these loading conditions are far from or close to the resonant ones and to predict a structural response at the resonant excitation. Such a problem is rather complicated because typically the 'initial' or 'original' shape of a flexible tube is quite different from the shape, which it has in a mounted device. Thus, before addressing dynamics of a flexible fluid-conveying tube, it is often necessary to solve a static problem of its nonlinear deformation.

There is large number of publications referred to dynamics of fluid-conveying tubes. The present state of affairs in this area is outlined by Paidoussis (1998). Most of the publications surveyed in this book are devoted to various aspects of vibrations of straight tubes, specifically in the cases, when a tube is clamped at both sides or it is clamped at one edge and free at the other. In a recent paper by Langthjem and Sugiyama (2000), a comprehensive survey of the literature devoted to the latter case is given. Some attention in Chapter 6 of the book by Paidoussis (1998) has been also paid to vibrations of curved pipes conveying fluid and the most useful classification of the approaches is given there as: (i) the conventional inextensible theory, (ii) the extensible theory, and (iii) the modified inextensible theory. The main point in

*Corresponding author.
E-mail address: sorokins@mail.ru (S.V. Sorokin).

0889-9746/03/$ - see front matter
PII: S0889-9746(02)00144-5

Nomenclature

a_1, b_1	parameters defining the distribution of moment of inertia
c_t	the velocity of sound in the tube material, equal to $\sqrt{E/\bar{\rho}}$
$\bar{D}(s)$	variable dimensional outer diameter of tube cross-section
$\bar{d}$	dimensional inner diameter of tube cross-section
d	nondimensional inner diameter of tube cross-section, equal to $\bar{d}/l$
E	Young's modulus
F	area of tube cross-section
F_{fl}	area occupied by a fluid
k	material constant defining its physical nonlinearity
l	dimensional length of a tube
$\bar{M}_i$	dimensional concentrated bending moment
M_i	nondimensional concentrated bending moment, equal to $\bar{M}_i/El\bar{d}^2$
p_0	dimensional static axial compressive force
$\bar{s}$	dimensional axial coordinate
s	nondimensional axial coordinate
β_0	nondimensional static axial compressive force equal to $p_0/E\bar{d}^2$
β_{cr}	nondimensional static buckling force $\pi^3 d^2(\alpha^4-1)/64$
γ	nondimensional modal damping coefficient
ε	formal nondimensional small parameter to indicate level of approximation
$\hat{\varepsilon}$	axial strain
$\bar{v}$	circular frequency of flow pulsation
v	nondimensional circular frequency of flow pulsation, equal to $\bar{v}/\omega_0$
$\bar{\rho}, \bar{\rho}_{fl}$	dimensional densities of a tube material and fluid, respectively
ρ	nondimensional fluid density, equal to $\bar{\rho}_{fl}/\bar{\rho}$
σ	nondimensional detuning parameter
$\hat{\sigma}$	axial stress
$\bar{\chi}_0$	dimensional mean flow velocity component
$\bar{\chi}_1$	dimensional amplitude of flow harmonic pulsation
χ_0	nondimensional mean flow velocity component, equal to $\bar{\chi}_0/c_t$
χ_1	nondimensional amplitude of flow harmonic pulsation, equal to $\bar{\chi}_1/c_t$
dot	time derivative, $\partial/\partial t$
prime	spatial derivative, $\partial/\partial s$.

this classification is related to the role of flow-induced changes in static equilibrium configuration of a tube. Apparently, this issue is most important when a pipe (say, a hose) is really flexible, i.e., when its bending stiffness is fairly small and flow velocity actually controls its shape. This also means that the 'initial' shape of a tube (the shape it has in the absence of a flow) is not 'pre-stressed' in all cases. However, in many practical situations, it is not entirely relevant and a tube may be stiff enough not to change its configuration in response to variations in mean flow velocity. On the other hand, it may be sufficiently flexible to exhibit a large static deformation due to action of some external forces or moments not produced by a fluid–structure interaction. Then dynamic characteristics of a tube (e.g., its eigenfrequencies and eigenmodes) are controlled by such the static deformation. The present paper addresses exactly this case. A standard nonlinear beam theory (a flexible rod with a nonextensible axis) is used and firstly a nonlinear static bending of an originally straight flexible elastic fluid-conveying tube having variable moment of inertia is considered. In this formulation, the static bending is not affected by the presence of a fluid. Secondly, linear vibrations of a tube are considered provided that fluid's flow does not modify a static shape of a tube, but convection of a fluid's mass makes corrections to tube's eigenfrequencies and eigenmodes of vibrations. Finally, nonlinear effects produced by a flow pulsation are studied.

A problem of nonlinear static bending is posed in two cases: (i) a tube loaded by super-critical axial compressive forces acting at its edges and (ii) a tube loaded by distributed bending moments specified as a function of the axial coordinate, in particular, as delta functions. In the present paper, deformations are considered which are symmetric with respect to the mid-span of a simply supported tube. A tube has a circular cross-section with a constant inner

diameter and a variable outer diameter. The nonlinearity produced by large displacements and slopes of a deformed tube is taken simultaneously into account with the nonlinearity in a strain–stress relation in an ideal elasticity of the tube's material. An equilibrium configuration is found by minimisation of the functional of a potential energy of a tube by the method of 'local variations' suggested by Banichuk and Tchernousko (1973). The analytical solution given by Euler's *elastica* for a tube of a uniform cross-section compressed by axial forces is used to validate this algorithm of numerical solution.

Analysis of dynamics is performed in Section 2 for 'in-plane' motions of a tube, i.e., those developed in the plane of static bending deformation. A nonlinear equation of vibrations of a fluid-conveying tube is derived in Section 3 by applying Hamilton's principle. A set of eigenfrequencies and relevant eigenmodes is found in a linearised formulation. Then in Section 4 bi-modal analysis of nonlinear vibrations is performed. The standard multiple scales method (see Nayfeh, 1973 or Thomsen, 1997) is applied to explore a case of the parametric excitation of vibrations by a flow pulsation.

2. The static problem of nonlinear bending

A practical formulation of the problem for an elastic flexible tube either compressed by a supercritical axial force or loaded by bending moments is to determine a distribution of bending moments (or a value of the supercritical compressive force) that provides its desired shape. This is an inverse problem formulation, which may be computationally quite expensive to solve. To avoid solving such a problem, an external loading may be considered as given, whereas stiffness and geometry parameters of a tube may be treated as subjected to possible changes (some scalar 'active' parameters of design should be introduced). Then a static problem of an 'initial design' for a tube loaded by given axial forces or bending moments should be solved first, and a sensitivity analysis of the shape of a tube (selected as an objective function) to the variations of parameters of design should be performed. Values of the design variables yielding the desired shape of a tube may be identified based on results of such a sensitivity analysis.

We consider nonlinear static bending of a tube provided that it is sufficiently slender so that no local buckling occurs and it preserves cylindrical shape of the tube inner cross-section along the whole length l (a dimensional axial coordinate $\bar{s}$ is introduced hereafter). It is also assumed that a pressure in the fluid does not affect static deformation of a tube, which therefore may be analysed without fluid loading. A beam of the tubular cross-section having a variable moment of inertia is considered and the latter is selected as

$$I(s) = \frac{\pi \bar{d}^4(\alpha^4(s) - 1)}{64}, \tag{1}$$

where $\alpha(s) = \bar{D}(s)/\bar{d}$, $\bar{D}(s)$ is variable dimensional outer diameter, $\bar{d} = \text{const}$ is the dimensional inner diameter of tube cross-section, $s = \bar{s}/l$ is the nondimensional axial coordinate. There is the evident constraint imposed on a function $\alpha(s)$:

$$\alpha(s) > 1.0. \tag{2}$$

We restrict our analysis to symmetric (with respect to mid-span) shapes of a deformed tube, so this function has to be symmetric too. The straightforward assumption then would be to choose a quadratic approximation. However, we consider the case when a function $\alpha(s)$ is specified as

$$\alpha_*(s) = a_1 \cos\left(\frac{2\pi s}{3} - \frac{\pi}{3}\right) + b_1, \tag{3}$$

where a_1, b_1 are some constants. Formula (3) provides rather smooth symmetric dependence of tube's moment of inertia on an axial coordinate. Of course, material distribution, given in this formula, is quite specific, but it features a typical case when a tube is softer at its ends, than at the middle. For example, if $a_1 = 0.2, b_1 = 0.9$, then the thickness of a tube tends to zero at its ends while the outer diameter at the middle of a beam exceeds in 10% the inner diameter. In fact, function (3) is fairly similar to quadratic polynomial, but it has appeared that from the viewpoint of efficiency of computations by *Mathematica* software (Wolfram, 1991), this shape function is more convenient.

A tube is made of a material exhibiting nonlinear elastic behaviour, and the following rheological law of nonlinear elasticity is adopted after Tchernykh (1978):

$$\hat{\sigma} = E\hat{\varepsilon}(1 - k\hat{\varepsilon}^2), \tag{4}$$

where $\hat{\sigma}, \hat{\varepsilon}$ are the axial stress and axial strain, respectively, E is Young's modulus and k is a material constant.

The equilibrium configuration of a tube is conveniently defined by the angle $\varphi(s)$ (see Fig. 1(a) for the case of compression by an axial force) selected as an unknown function of a 'material' coordinate s. The following energy functional is introduced (see Banichuk and Tchernousko, 1973):

$$J = \int_0^1 \left\{ \frac{\pi d^2}{2} (\varphi_0')^2 \left[\frac{\alpha^4 - 1}{64} - \frac{k d^2 (\alpha^6 - 1)}{512} (\varphi_0')^2 \right] + \beta_0 \cos \varphi_0 + \sum_i M_i \varphi_{0i} \delta(s - s_i) \right\} \mathrm{d}s, \tag{5}$$

where $\delta(s - s_i)$ is the Dirac delta function and primes denote the spatial derivative $\partial/\partial s$.

The stationarity condition for this functional defines the stable equilibrium configuration of the tube. The first term in square brackets presents contribution to the potential energy from the linear component in (4), the second one is related to the nonlinear component. Formulation (5) comprises both the loading by an axial compressive force (the second term) and the loading by bending moments (the third term). It is written in the nondimensional form (the energy functional is scaled to $El\bar{d}^2$). In functional (5), $\beta_0 = p_0/E\bar{d}^2$ is a value of the nondimensional static axial compressive force, $d = \bar{d}/l$ is the ratio of the inner diameter to the length of the tube and $M_i = \bar{M}_i/Eld^2$ is the nondimensional bending moment at the point $s = s_i$. Variation of an energy functional (5) with respect to function $\varphi_0(s)$ results in the following differential equation:

$$\beta_0 \sin \varphi_0 + \frac{\pi d^2}{64} \left[\varphi_0' (\alpha^4 - 1) \right]' - \frac{k \pi d^4}{256} \left[(\varphi_0')^3 (\alpha^6 - 1) \right]' + \sum_i M_i \delta_i (s - s_i) = 0. \tag{6}$$

For a simply supported tube, a condition

$$\int_0^1 \sin \varphi_0(s) \, \mathrm{d}s = 0 \tag{7}$$

which implies a lateral deflection of a tube $w_0(s)$ should vanish at the right edge is used. An analytical solution for the boundary problem (6), (7) is not available for arbitrary function $\alpha(s)$ and numerical algorithm suggested by Banichuk and Tchernousko (1973) is used. It is not a goal of this paper to give detailed description of this algorithm, but it is appropriate to note that it is based on discretisation of the function $\varphi_0(s)$ at nodal collocation points and successive perturbations of its values there. This procedure is rather complicated and time-consuming in the general case. However, it is considerably simplified if a deformed tube remains symmetric with respect to its middle cross-section. In all the cases considered in this paper the symmetry condition holds true and therefore the numerical algorithm is computationally inexpensive.

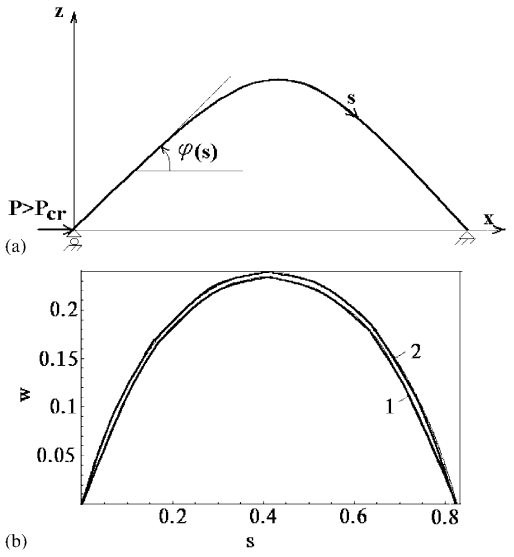

Fig. 1. (a) A buckled tube and (b) buckled configuration of an axially compressed tube: curve 1—exact solution; curve 2—numerical solution.

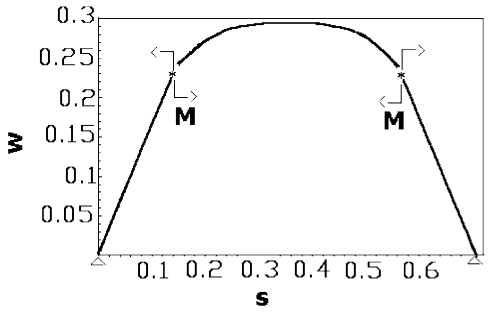

Fig. 2. A deformed tube symmetrically loaded by concentrated bending moments.

To check the validity of this numerical procedure, the computed shape of a buckled beam has been compared with the available analytical results. Problem (6), (7) has a well-known solution in the case of an axially compressed beam for $\alpha(s) = \text{const}$. The elementary linear stability analysis gives a static buckling force $\beta_{cr} = \pi^3 d^2(\alpha^4 - 1)/64$, and the nonlinear analysis of buckling gives a post-critical ($\beta_0 > \beta_{cr}$) configuration of a tube as Euler's *elastica*. As the function $\varphi(s)$ is found, a nondimensional lateral displacement $w(s)$ and a corresponding horizontal coordinate $x(s)$ are readily computed

$$\begin{aligned} w(s) &= \int_0^s \sin\varphi(s)\,\mathrm{d}s, \\ x(s) &= 1 - \int_s^1 \cos\varphi(s)\,\mathrm{d}s. \end{aligned} \tag{9}$$

In Fig. 1(b), curve 1 represents buckled configuration of a tube corresponding to Euler's *elastica* for $\alpha(s) = 1.5$, $d = 0.02$, $\beta_{st} = 1.1\beta_{cr}$, e.g., an exact solution in the form of elliptic integrals, see, for example, Timoshenko (1936). Curve 2 represents the equilibrium shape of the same tube obtained by Banichuk–Tchernousko algorithm for 1024 collocation points introduced along the length of a tube. The equilibrium shape of the beam obtained for 2048 collocation points is exactly the same as displayed by curve 2, which witnesses a convergence of this algorithm. There is a good agreement between curves 1 and 2, and hence all results reported below are obtained provided that the static problem is solved at this level of approximation. In Fig. 2, the equilibrium shape of the same tube loaded by two symmetrically positioned ($s_M = 0.25$ and 0.75) concentrated moments ($M = 5.32 \times 10^{-4}$) is shown. Apparently, a tube is deformed only between the points where moments are applied, while its 'outer' parts remain straight.

In Figs. 3(a) and (b), static equilibrium configurations of the tube with a nonuniform cross-section are shown. It is loaded by two moments at $s_M = 0.25$ and 0.75. The results illustrated in Fig. 3(a) are obtained for the following set of parameters of design: $a_1 = 0.4$, $M = 1.73 \times 10^{-3}$, $k = 0.2$, and $d = 0.05$. Three values of parameter b_1 are taken and as is seen, the deformed shape of a tube is very sensitive to possible variations of design parameters. In Fig. 3(b), the static configuration of a beam is shown for $b_1 = 0.9$, $k = 0.2$ in two loading cases. Although the magnitudes of bending moment M and tube parameter a_1 are different, maximum lateral deflection in both cases is approximately the same ($w_{\max}/l = 0.365$). Thus, a proper choice of design parameters controlling moment of inertia (a_1, b_1) in response to alternations in a bending moment (M) may fulfil the required constraints imposed on deflections of a tube (if there are any). The role of a nonlinear elasticity is illustrated in Fig. 4 for the case of $M = 8.96 \times 10^{-5}$ (two moments are positioned at $s_M = 0.25$ and 0.75), $d = 0.02$, $a_1 = 0.2$, and $b_1 = 0.9$. Curve 1 presents an equilibrium configuration of the beam obtained with the nonlinear elasticity term included into Hamiltonian ($k = 0.2$), curve 2 corresponds to analysis performed with $k = 0$. As is seen, the difference between these two curves is negligibly small. In fact, the nonlinear elasticity plays an important role only for rather short rods, i.e., when the ratio of an inner diameter of the tube to its length is not very small. For such short tubes large 'global' bending is typically associated with local buckling which is not considered in this paper. Therefore, we conclude that the dominant nonlinear effect in behaviour of long tubes is produced by a nonlinear geometry, rather than by a nonlinear constitutive law.

3. Governing equations of motions of a deformed tube: linear analysis of vibrations

The dynamics of a tube is considered in the case when it has been subjected to large static deformation and then a fluid flow is introduced. It is convenient to use Hamilton's principle to derive governing equations of motions.

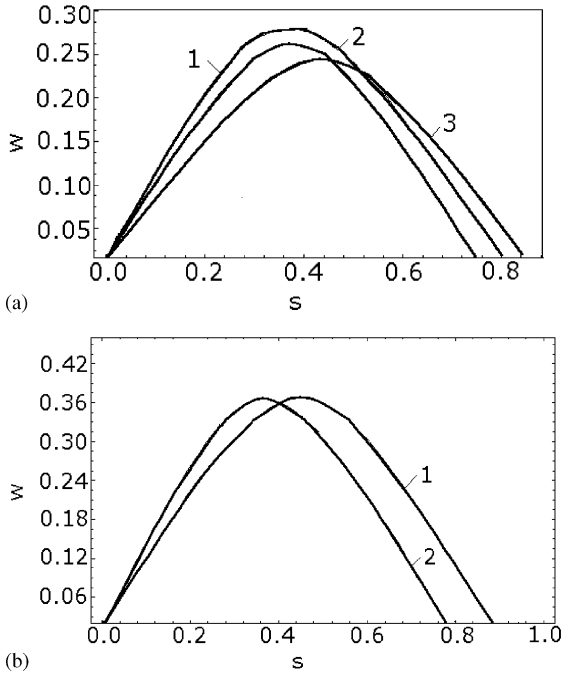

Fig. 3. (a) Static deformation of a tube with a nonuniform cross-section loaded by two moments. Influence of design parameter b_1: curve 1—$b_1 = 0.8$; curve 2—$b_1 = 0.95$; curve 3—$b_1 = 1.0$ and (b) static deformation of a tube with a nonuniform cross-section loaded by two moments. Curve 1—$M = 5.82 \times 10^{-4}$, $a_1 = 0.30$; curve 2—$M = 5.41 \times 10^{-4}$, $a_1 = 0.22$.

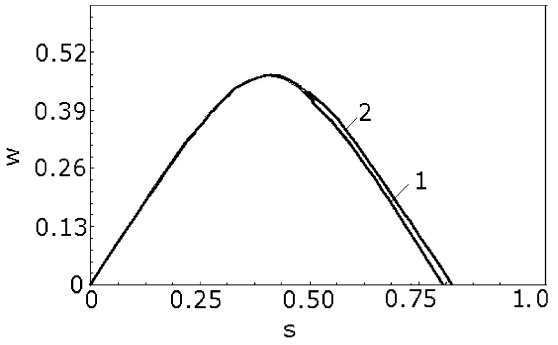

Fig. 4. Static deformation of a tube with a nonuniform cross-section loaded by two moments. Role of nonlinear elasticity. Curve 1—$k = 0.2$; curve 2—$k = 0$.

The potential energy of a tube and its kinetic energy are presented in the dimensional form as

$$V = \frac{EI(\bar{s})}{2}(\varphi')^2 - Ek\pi\frac{\bar{D}^6(\bar{s}) - \bar{d}^6}{1024}(\varphi')^4,$$
$$K = \frac{\bar{\rho}F}{2}((\dot{u})^2 + (\dot{w})^2) + \frac{\bar{\rho}_{fl}F_{fl}}{2}((\dot{u} + \bar{\chi}\cos\varphi)^2 + (\dot{w} + \bar{\chi}\sin\varphi)^2), \tag{10}$$

where $\bar{\rho}, \bar{\rho}_{fl}$ are densities of the tube material and fluid, respectively, F is the cross-sectional area of the tube, F_{fl} is the area occupied by the fluid, and dots denote a time derivative. The flow velocity is introduced in the form

$$\bar{\chi} = \bar{\chi}_0 + \bar{\chi}_1 \cos\bar{\nu}t, \tag{11}$$

$\bar{\chi}_0, \bar{\chi}_1$ are the mean flow velocity component and the amplitude of its harmonic pulsation, respectively, $\bar{\nu}$ is a circular frequency of flow pulsation. As is seen from (10), the flow of an incompressible inviscid fluid contributes only to the kinetic energy of a system, so we have assumed that the gravity force is neglected or a horizontal tube is considered. We also assume that the axis of a tube is incompressible and its axial displacement is formulated as,

$$u(\bar{s}) = l - \bar{s} - \int_{\bar{s}}^{l} \cos\varphi \, \mathrm{d}\bar{s}. \tag{12}$$

The Hamiltonian becomes

$$H = \int_0^l \int_{t_1}^{t_2} \left\{ -\frac{EI(\bar{s})}{2}(\varphi')^2 + Ek\pi\frac{\bar{D}^6 - \bar{d}^6}{1024}(\varphi')^4 + \frac{\bar{\rho}F}{2}\left[\left(\int_{\bar{s}}^{l} \dot{\varphi}\sin\varphi \, \mathrm{d}\bar{s}\right)^2 + \left(\int_0^{\bar{s}} \dot{\varphi}\cos\varphi \, \mathrm{d}\bar{s}\right)^2\right] \right.$$
$$\left. + \frac{\bar{\rho}_{fl}F_{fl}}{2}\left[\left(\int_{\bar{s}}^{l} \dot{\varphi}\sin\varphi \, \mathrm{d}\bar{s} + \bar{\chi}\cos\varphi\right)^2 + \left(\int_0^{\bar{s}} \dot{\varphi}\cos\varphi \, \mathrm{d}\bar{s} + \bar{\chi}\sin\varphi\right)^2\right]\right\} \mathrm{d}t \, \mathrm{d}\bar{s}. \tag{13}$$

The stationarity condition $\delta H + \int_{t_1}^{t_2} \delta W_p \, \mathrm{d}t + \int_0^l \int_{t_1}^{t_2} \delta A \, \mathrm{d}t \, \mathrm{d}\bar{s} = 0$ yields the nonlinear equation of motions

$$\int_0^{\bar{s}_2}\left[(\bar{\rho}F + \bar{\rho}_{fl}F_{fl})\int_0^{\bar{s}_1}(\ddot{\varphi}\cos\varphi - (\dot{\varphi})^2\sin\varphi)\,\mathrm{d}\bar{s}_1\right]\mathrm{d}\bar{s}_2\cos\varphi$$
$$- \int_0^{\bar{s}_2}\left[(\bar{\rho}F + \bar{\rho}_{fl}F_{fl})\int_{\bar{s}_1}^{l}(\ddot{\varphi}\sin\varphi + (\dot{\varphi})^2\cos\varphi)\,\mathrm{d}\bar{s}_1\right]\mathrm{d}\bar{s}_2\sin\varphi$$
$$+ \bar{\rho}_{fl}\bar{F}_{fl}\left[\int_0^{\bar{s}}(\dot{\bar{\chi}}\sin\varphi + 2\bar{\chi}\dot{\varphi}\cos\varphi)\,\mathrm{d}\bar{s}\cos\varphi - \int_0^{\bar{s}}(\dot{\bar{\chi}}\cos\varphi - 2\bar{\chi}\dot{\varphi}\sin\varphi)\,\mathrm{d}\bar{s}\sin\varphi\right]$$
$$+ (EI\varphi')' + p_0\sin\varphi + \frac{Ek\bar{d}^6\pi}{256}[(\varphi')^3(\alpha^6 - 1)]' + \sum_i \frac{\bar{M}_i}{l}\delta(\bar{s}/l - \bar{s}_i/l)$$
$$+ \bar{\rho}_{fl}F_{fl}\bar{\chi}^2\cos\varphi(0)\sin\varphi = 0. \tag{14}$$

Here the variation of a virtual nonconservative work is

$$\delta W_p = -\bar{\rho}_{fl}F_{fl}(\dot{u})^2\left(l - \int_{\bar{s}}^{l}\sqrt{1-(w')^2}\,\mathrm{d}\bar{s}\right)'\Bigg|_0 \delta\left(\int_{\bar{s}}^{l}\sqrt{1-(w')^2}\,\mathrm{d}\bar{s}\right)\Bigg|_0,$$

see Semler et al. (1994), and the work done by external potential forces is

$$A = \left[p_0(l-\bar{s}) - p_0\int_{\bar{s}}^{l}\cos\varphi\,\mathrm{d}\bar{s}\right]\Bigg|_{\bar{s}=0} + \sum_i \bar{M}_i\varphi_i\delta(\bar{s} - \bar{s}_i).$$

Eq. (14) is equally valid for the linear pre- and post-critical analysis of vibrations, for the analysis of nonlinear oscillations about buckled static configuration and for the analysis of large amplitude oscillations, including snap-through motions. It is convenient to transform Eq. (14) to a nondimensional form by introducing the following nondimensional parameters (besides those already used in Eq. (5)):

$$\tau = t\omega_0, \quad \lambda = \omega/\omega_0, \quad c_t = \sqrt{E/\bar{\rho}}, \quad \rho = \bar{\rho}_{fl}/\bar{\rho}, \quad \chi = \bar{\chi}/c_t,$$

where c_t is a sound speed in the tube material and ω_0 is a scaling factor for the time dependence. In an elementary linear analysis, this parameter is normally chosen as the first eigenfrequency of free oscillations of an unloaded tube. To analyse vibrations of a deformed tube, the function $\varphi(s,\tau)$ is formulated as

$$\varphi(s,\tau) = \varphi_0(s) + \tilde{\varphi}_1(s,\tau) \equiv \varphi_0(s) + \varphi_1(s)\exp(-\mathrm{i}\lambda\tau) \tag{15}$$

In Eq. (15), the function $\varphi_0(s)$ defines symmetric static equilibrium configuration and $\tilde{\varphi}_1(s,\tau)$ is the function describing small oscillations of a deformed tube. If formula (15) is substituted into Eq. (14) and linearisation with respect to

$\tilde{\varphi}_1(s,\tau)$ is performed, then one obtains

$$\beta_0\varphi_1\cos\varphi_0+\frac{\pi d^2}{64}\left[\varphi_1''(\alpha^4-1)+4\alpha^3\alpha'\varphi_1'\right]-\frac{k\pi d^4}{256}\left[18\alpha^5\alpha'(\varphi_0')^2\varphi_1'+3(\alpha^6-1)\left((\varphi_0')^2\varphi_1''+2\varphi_0'\varphi_0''\varphi_1'\right)\right]+\frac{\pi}{4}\rho\chi_0^2\varphi_1\cos\varphi_0\cos\varphi_0(0)+\frac{\pi}{4}\lambda^2\left[\int_0^s(\alpha^2-1+\rho)\int_0^s\varphi_1\cos\varphi_0\,\mathrm{d}s^2\cos\varphi_0-\int_0^s(\alpha^2-1+\rho)\int_s^1\varphi_1\sin\varphi_0\,\mathrm{d}s^2\sin\varphi_0\right]+\frac{\pi}{2}\rho\lambda\chi_0\left[\int_0^s\varphi_1\cos\varphi_0\,\mathrm{d}s\cos\varphi_0+\int_0^s\varphi_1\sin\varphi_0\,\mathrm{d}s\sin\varphi_0\right]=0. \tag{16}$$

In the case of a simply supported tube, the function $\varphi_1(s)$ is sought in the form

$$\varphi_1(s)=\sum_{m=1}^{N}A_m\cos m\pi s. \tag{17}$$

Eq. (16) is valid for computation of eigenfrequencies and eigenmodes of a tube containing a flowing fluid, since the fluid flow parameters χ_0,ρ are accounted for.

In this paper, the analysis of the statics and dynamics of the tube is performed in a nondimensional form, and its results could be applied to tubes of very different dimensions. However, as has already been discussed, our choice of parameters is aimed at modelling dynamics of rather small tubes made of rubber-like material and filled by water or another dense and weakly compressible fluid, which are used in the chemical industry or medical equipment.

The first and the second eigenfrequencies of an axially compressed tube having $\alpha(s)=\alpha_*(s)$, $a_1=0.2$, $b_1=0.9$, $d=0.02$ and $k=0.2$ are shown in Fig. 5(a). Curves 1 and 2 correspond to $\chi_0=0,\rho=0$, i.e., to the absence of a fluid and curves 3 and 4 correspond to $\chi_0=0,\rho=0.1$. As is well known, eigenfrequency parameters $(\omega_1 l/c_t)^2$ and $(\omega_2 l/c_t)^2$ in the pre-critical range $[0,\beta_{cr}]$ decay linearly with a growth in the magnitude of a compressive axial force, whereas in the post-critical range both of them grow relatively slowly with a supercritical growth in this force. In Fig. 5(b), the first two nondimensional eigenfrequency parameters of a tube loaded by concentrated bending moments acting at points $s_m=0.25$ and 0.75 are displayed as functions of the magnitude of a nondimensional bending moment M in the same manner as in Fig. 5(a). Unlike the case of loading by an axial force, an increase in the magnitude of bending moment results in monotonous growth of both frequencies. As follows from Figs. 5(a) and (b), various values of the ratio

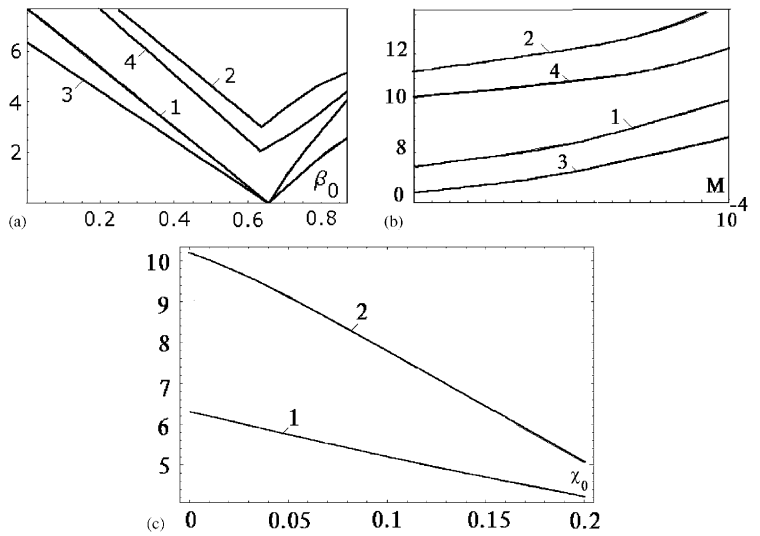

Fig. 5. (a) Dependence of the first two eigenfrequency parameters of a tube on the magnitude of a compressive axial force. Curves 1 and 3 display $(\omega_1 l/c_t)^2$; curves 2 and 4 display $(\omega_2 l/c_t)^2$, (b) dependence of the first two eigenfrequency parameters of a tube on the magnitude of a bending moments. Curves 1 and 3 display $(\omega_1 l/c_t)^2$; curves 2 and 4 display $(\omega_2 l/c_t)^2$, and (c) the first two eigenfrequency parameters of a tube loaded by concentrated bending moments as functions of the mean flow velocity χ_0. Curve 1—$(\omega_1 l/c_t)^2$; curve 2—$(\omega_2 l/c_t)^2$.

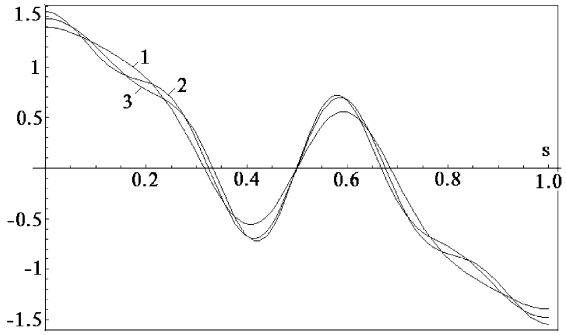

Fig. 6. The first eigenmode of a tube loaded by concentrated bending moments. Curve 1—four terms are retained in expansion (17); curve 2—five terms are retained; curve 3—six terms are retained.

between the first two eigenfrequencies (e.g., internal parametric resonance) may be obtained by a proper choice of magnitudes of an axial compressive force and bending moments. Fig. 5(c) shows the dependence of the first and the second eigenfrequency parameters on the mean component of flow velocity χ_0 for $\alpha(s) = \alpha_*(s)$, $a_1 = 0.2$, $b_1 = 0.9$, $d = 0.02,, k = 0.2$, $\rho = 0.1$ and static configuration relevant to $M = 2.99 \times 10^{-5}$. Both the eigenfrequency parameters decrease with the growth in χ_0 and it is in a good agreement with the results reported, for example, in Svetlitskij (1987). As follows from comparison of the graphs shown in Figs. 5(b) and (c), for a given range of parameters, eigenfrequencies decrease with growth in the mean component of flow velocity and increase with a growth in the static loading by bending moments.

As is well known, in the case of a simply supported axially loaded tube with constant outer and inner diameters, each eigenmode of vibrations is defined by a single term in expansion (17). If a tube has variable outer diameter, then it is necessary to retain several terms in (17) to construct each eigenmode. In Fig. 6 the first eigenmode is shown for a tube with the following set of parameters: $a_1 = 0.2$, $b_1 = 0.9$, $d = 0.02$ and $k = 0.2$. Bending moments of $M = 2.99 \times 10^{-5}$ are applied at $s_M = 0.25$ and 0.75. This eigenmode is a rather smooth function between tube end supports and loading points ($s < 0.25$ and $s > 0.75$). The static equilibrium shape of a deformed tube is a straight line in these regions. Between loading points, in the interval $0.25 < s < 0.75$, static bending occurs and the first eigenmode also varies with a high gradient. As is seen from comparison of these three curves, it is sufficient to retain five terms in expansion (17) to describe this eigenmode adequately.

4. Nonlinear dynamics: weak excitation

We consider near-resonant excitation of vibrations of a tube generated by flow pulsation and assume that the flow velocity has a mean and a pulsating component (11). In practical applications, such an excitation may be relevant to, say, pumping of a gasoline at a petrol station from a container to a car tank through a very flexible tube; or, in medicine, to blood convection through an artificial vessel. In these (and many other) cases fluid transportation is performed with some mean flow velocity subjected to small variations. Apparently, if the frequency of flow pulsation is fairly close to the resonant frequency, then undesirable nonlinear phenomena may occur in the single-mode regime of motions. It is also possible that, besides the coincidence between a frequency of flow pulsation with the first eigenfrequency, there also exists an internal parametric resonance between the first two eigenfrequencies. Then a nonlinear interaction between vibrations at these two eigenmodes (which are symmetric and skew symmetric, respectively) may develop and result in dangerous bi-modal regimes of large-amplitude motions. In this section, we consider both cases.

The standard approach we adopt to solve this problem governed by nonlinear partial differential Eq. (14) is to combine Galerkin method for the spatial coordinate with a method of multiple scales, to obtain an analytical solution of a reduced system of nonlinear ordinary differential 'modal' equations in the time domain. A set of linear eigenmodes is used in the spatial coordinate. Direct numerical integration of the original Eq. (14) involves discretisation in the space and time domains and, therefore, cannot give a clear insight into nonlinear effects of modal interaction due to the inevitable presence of, for example, round-off errors. Therefore, analytical predictions obtained by the use of a method of multiple scales are validated in this section by comparison with results of numerical integration of a reduced system of 'modal' nonlinear ordinary differential equations in time.

4.1. Single-mode analysis. Primary resonance

The method of multiple scales (Nayfeh, 1973; Thomsen, 1997) is used and a time-dependent component of function $\tilde{\varphi}_1(s,\tau)$ is sought similarly to (15) as

$$\tilde{\varphi}_1(s,\tau) = A(\tau)\varphi_1(s), \tag{18}$$

i.e., as a product of a shape function $\varphi_1(s)$, taken here as the first eigenmode of linear oscillations about the post-critical static equilibrium configuration, and a function $A(\tau)$ pertaining to the time dependence. Such a choice of a function $\tilde{\varphi}(s,\tau)$ is standard in analysis of near-resonant nonlinear vibrations. It should be emphasised here that the eigenmode $\varphi_1(s)$ depends on the static equilibrium shape of a tube and on the mean flow velocity, as shown in the previous section. If, for example, static bending moments acting at the tube are changed, then this function should be modified because a solution of the problem in static bending $\varphi_0(s)$ is also changed.

The method of multiple scales allows the solution of Eq. (14) to be rewritten as function of independent time variables (scales). Thus, if τ is rewritten as $T_0 = \tau$, then a 'slow' time is introduced as $T_1 = \varepsilon\tau$ (ε serves only to indicate level of approximation) and the time derivative becomes $\mathrm{d}/\mathrm{d}\tau = \partial/\partial T_0 + \varepsilon\partial/\partial T_1$. An excitation (flow pulsation) is formulated in the nondimensional form as $\chi = \chi_0 + \varepsilon\chi_1 \cos \nu\tau$, $\nu = \bar{v}/\omega_0$. An asymptotic solution can now be expressed in the form

$$A(\tau) = B_0(T_0, T_1) + \varepsilon B_1(T_0, T_1). \tag{19}$$

The fast scale describes oscillations in 'real time', while the slow time T_1 accounts for slow modulations of amplitudes and phases. The above formulation with two time scales is applied to study nonlinear motions of the tube under external parametric resonance excitation conditions. Then the governing equation of motion (14) is transformed to a polynomial form, up to the cubic powers of $A(\tau)$. Galerkin's orthogonalisation procedure is applied, with the first eigenmode $\varphi_1(s)$ used as a trial function, and the resulting ordinary differential nonlinear equation of motion is (hereafter, $\lambda \equiv \lambda_1$ unless otherwise is stated)

$$\begin{aligned} k_1\ddot{A} + k_2 A = {} & k_3A^2 + k_4A^3 + \rho\chi_0\chi_1\left(k_8 + k_9A + k_{10}A^2\right)\cos\nu\tau + \rho\chi_1^2(k_{11} + k_{12}A)\cos^2\nu\tau \\ & + \nu\rho\lambda_1\chi_1\left(k_{13} + k_{14}A + k_{15}A^2\right)\sin\nu\tau + \rho\lambda_1\chi_1\left(k_{16}\dot{A} + k_{17}A\dot{A}\right)\cos\nu\tau \\ & + \rho\lambda_1\chi_0\left(k_{18}\dot{A} + k_{19}A\dot{A} + k_{20}A^2\dot{A}\right) + \lambda_1^2\left(k_{21}(\dot{A})^2 + k_{22}A(\dot{A})^2 + k_{23}A\ddot{A} + k_{24}A^2\ddot{A}\right) - \gamma\dot{A}, \end{aligned} \tag{20}$$

where $k_i (i = 1, 2, \ldots, 24)$ are coefficients depending on functions $\varphi_0(s)$ and $\varphi(s)$, see Appendix A and γ is a nondimensional modal damping coefficient. This parameter is introduced to take into account the energy dissipation in the tube material. Here we adopt the simple assumption that the dissipation does not depend on the frequency of excitation and on the mode shape. It should be pointed out that flow-induced 'damping' is accounted for in this model by the term $\rho\lambda_1\chi_0 k_{18}A^{\cdot}$ in Eq. (20). Apparently, the first eigenfrequency of oscillations may be formulated as $\lambda_1 = \sqrt{k_2/k_1}$. We consider a resonant case and let the excitation frequency be defined as

$$\nu = \lambda_1 + \varepsilon\sigma, \tag{21}$$

where the detuning parameter σ serves to indicate a mismatch between the frequencies v and λ_1.

Then equation of motion (20) may conveniently be split into two equationsto order ε^0:

$$\frac{\partial^2 B_0}{\partial T_0^2} + \lambda_1^2 B_0 = 0, \tag{22}$$

and to order ε^1:

$$\begin{aligned} \frac{\partial^2 B_1}{\partial T_0^2} + \lambda_1^2 B_1 = {} & \frac{1}{k_1}\Bigg[-2k_1\frac{\partial^2 B_0}{\partial T_0 \partial T_1} + k_3B_0^2 + k_4B_0^3 + \rho\chi_0\chi_1(k_8 + k_9B_0 \\ & + k_{10}B_0^2)\cos\nu T_0 + \rho\chi_1^2(k_{11} + k_{12}B_0)\cos^2\nu T_0 + \nu\rho\lambda_1\chi_1(k_{13} + k_{14}B_0 + k_{15}B_0^2)\sin\nu T_0 \\ & + \rho\lambda_1\chi_1(k_{16} + k_{17}B_0)\frac{\partial B_0}{\partial T_0}\cos\nu T_0 + \rho\lambda_1\chi_0(k_{18} + k_{19}B_0 + k_{20}B_0^2)\frac{\partial B_0}{\partial T_0} \\ & + \lambda_1^2\left(k_{21}\left(\frac{\partial B_0}{\partial T_0}\right)^2 + k_{22}B_0\left(\frac{\partial B_0}{\partial T_0}\right)^2 + k_{23}B_0\frac{\partial^2 B_0}{\partial T_0^2} + k_{24}B_0^2\frac{\partial^2 B_0}{\partial T_0^2}\right) - \gamma\frac{\partial B_0}{\partial T_0}\Bigg]. \end{aligned} \tag{23}$$

The first term in the asymptotic expansion (19) is a solution of Eq. (22) and it has the form

$$B_0 = N(T_1)\exp(\mathrm{i}\lambda_1 T_0) + \hat{N}(T_1)\exp(-\mathrm{i}\lambda_1 T_0), \tag{24}$$

where the second term is the complex conjugate of the first one. To obtain a uniformly valid asymptotic solution, the secular terms in the fast time scale T_0 must be eliminated from the right-hand side of Eq. (23). Solution in the slow time is sought as $N(T_1) = \frac{1}{2}a(T_1)\exp(\mathrm{i}\xi(T_1))$; here $a(T_1)$ and $\xi(T_1)$ are its real-valued amplitude and phase, respectively. Substituting (24) in (23), eliminating the secular terms, and separating the real and imaginary parts gives the following system of amplitude modulation equations:

$$\frac{\mathrm{d}a}{\mathrm{d}T_1} = \frac{1}{2\lambda_1}\left\{\left[-\rho\chi_0\chi_1\left(\frac{k_8}{2}+k_0a^2\right) - v\rho\lambda_1\chi_1\frac{k_{13}}{2} + \rho\chi_0\chi_1a^2\frac{k_{10}}{2} - v\rho\lambda_1\chi_1a^2\frac{3k_{15}}{2}\right]\sin\psi \right.$$
$$\left. +\lambda_1^2\rho\chi_0a^3k_{20} - \rho\chi_1^2\frac{k_{12}}{4}\sin 2\psi + \lambda_1^2\rho\chi_1\frac{a^2}{2}k_{17}\cos\psi + \lambda_1^2\rho\chi_0k_{18}a - \gamma\lambda_1a\right\}, \tag{25}$$

$$a\frac{\mathrm{d}\psi}{\mathrm{d}T_1} = -\frac{1}{2\lambda_1}\left\{\left[\rho\chi_0\chi_1\left(\frac{k_8}{2}+k_{10}a^2\right) + v\rho\lambda_1\chi_1\frac{k_{13}}{2} + \rho\chi_0\chi_2\frac{k_{10}}{2}a^2 + v\rho\chi_1\frac{k_{15}}{2}a^2\right]\cos\psi \right.$$
$$+\frac{\rho\chi_1^2}{2}ak_{12} + \rho\chi_1^2\frac{k_{12}}{4}\cos 2\psi - \lambda_1^2\rho\chi_1a^2\frac{k_{17}}{2}\sin\psi$$
$$\left.+(3k_4+\lambda_1^2k_{22}\lambda^2 - 3\lambda_1^2k_{24}\lambda^2)a^3 + 2a\lambda_1\sigma\right\},$$

where another phase angle is introduced as $\psi = \xi - \sigma T_1$. The derivative of a phase angle ξ becomes

$$\mathrm{d}\xi/\mathrm{d}T_1 = \mathrm{d}\psi/\mathrm{d}T_1 + \sigma T_1. \tag{26}$$

A stationary amplitude of a is obtained from Eq. (25) by letting $\mathrm{d}a/\mathrm{d}T_1 = a(\mathrm{d}\psi/\mathrm{d}T_1) = 0$ and solving a system of nonlinear equations with respect to a and ψ. Then stability of this solution is checked in a standard way (see, for example, Nayfeh, 1973) by constructing the Jacobian of system (25) and calculating its eigenvalues at the stationary point. Negative real parts of all eigenvalues indicate stability of the obtained solution.

Typical amplitude response curves are presented in Fig. 7 for perfectly tuned weak resonant excitation. A tube is statically loaded by two moments of magnitude $M = 2.21\times10^{-5}$ applied at $s_m = 0.25$ and 0.75. The parameters of the tube are: $a_1 = 0.2$, $b_1 = 0.95$, $d = 0.02$, $k = 0.2$ and $\gamma = 0.1$. The nondimensional density of the fluid is ($\rho =$) 0.2. The amplitude of symmetric resonant vibrations is plotted versus pulsating component of flow velocity χ_1 for two values of mean flow velocity χ_0. Solid lines present a stable solution of amplitude modulation Eq. (25), while circles designate values of the amplitude a obtained by direct numerical integration of the 'modal' Eq. (20). As is seen, for small flow pulsation, the zero solution is stable and no flexural motions develop. However, as the amplitude of flow pulsation reaches a certain threshold value, the zero solution loses stability and the tube performs nonlinear vibrations. As is seen, the mean flow component produces a stabilising effect on the dynamic behaviour of the system.

4.2. Bi-modal analysis: internal parametric resonance

In the previous part of the paper, resonant excitation has been considered provided that only condition (21) holds. However, as suggested by the analysis of linear vibrations of a tube, it is possible that besides this condition, an internal

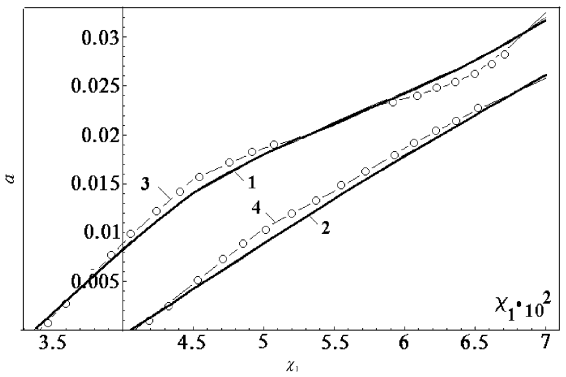

Fig. 7. Amplitude response curves (a perfectly tuned resonance) versus a magnitude of pulsating flow component χ_1. Mean flow velocity $\chi_0 = 0.1$ (curves 1 and 3) and $\chi_0 = 0.2$ (curves 2 and 4).

parametric resonance occurs, i.e.,

$$\lambda_2 = 2\lambda_1 + \varepsilon\sigma_2, \tag{27}$$

where λ_2 is the second eigenfrequency of oscillations about the buckled static equilibrium position. As before, the flow velocity is given as $\chi = \chi_0 + \varepsilon\chi_1 \cos v\tau$. The solution of a problem is sought now as

$$\varphi(s,\tau) = \varphi_0(s) + C_1(\tau)X_1(s) + C_2(\tau)X_2(s), \tag{28}$$

where $X_1(s), X_2(s)$ are selected as the first and second eigenmodes of the tube conveying fluid with constant velocity. Standard Galerkin orthogonalisation technique gives two ordinary differential equations ($\lambda \equiv \lambda_1$):

$$\begin{aligned}
&a_1\ddot{C}_1 + a_3\dot{C}_1 + a_4\dot{C}_2 + a_5C_1 = a_7C_1^2 + a_8C_2^2 + a_9C_1C_2\\
&\quad + a_{10}C_1^2C_2 + a_{11}C_1C_2^2 + a_{12}C_1^3 + a_{13}C_2^3 + \chi_1\rho\chi_0(a_{14} + a_{15}C_1 + a_{16}C_2\\
&\quad + a_{17}C_1C_2 + a_{18}C_1^2 + a_{19}C_2^2)\cos v\tau + \rho\chi_1^2(a_{20} + a_{21}C_1 + a_{22}C_2)\cos^2 v\tau\\
&\quad + v\rho\lambda\chi_1(a_{23} + a_{24}C_1 + a_{25}C_2 + a_{26}C_1^2 + a_{27}C_2^2 + a_{28}C_1C_2)\sin v\tau\\
&\quad + \rho\lambda\chi_1(a_{29}\dot{C}_1 + a_{30}\dot{C}_2 + a_{31}C_1\dot{C}_1 + a_{32}C_1C_2 + a_{33}C_1\dot{C}_2 + a_{34}C_2\dot{C}_2\\
&\quad + a_{35}C_2\dot{C}_1)\cos v\tau + \rho\lambda\chi_0[(a_{36} + a_{37}C_1 + a_{38}C_2 + a_{39}C_1C_2)\dot{C}_1\\
&\quad + (a_{40} + a_{41}C_1 + a_{42}C_2 + a_{43}C_1C_2)\dot{C}_2 + \lambda^2(a_{44}\dot{C}_1^2 + a_{45}\dot{C}_1\dot{C}_2 + a_{46}\dot{C}_2^2\\
&\quad + a_{47}C_1\dot{C}_1^2 + a_{48}C_2\dot{C}_2^2 + a_{49}C_1\ddot{C}_1 + a_{50}C_2\ddot{C}_2 + a_{51}C_1^2\ddot{C}_1 + a_{52}C_2^2\ddot{C}_2) - \gamma\dot{C}_1,
\end{aligned} \tag{29a}$$

$$\begin{aligned}
&b_2\ddot{C}_2 + b_4\dot{C}_2 + b_3\dot{C}_1 + b_6C_2 = b_7C_1^2 + b_8C_2^2 + b_9C_1C_2\\
&\quad + b_{10}C_1^2C_2 + b_{11}C_1C_2^2 + b_{12}C_1^3 + b_{13}C_2^3 + \chi_1\rho\chi_0(b_{14} + b_{15}C_1 + b_{16}C_2\\
&\quad + b_{17}C_1C_2 + b_{18}C_1^2 + b_{19}C_2^2)\cos v\tau + \rho\chi_1^2(b_{20} + b_{21}C_1 + b_{22}C_2)\cos^2 v\tau\\
&\quad + v\rho\lambda\chi_1(b_{23} + b_{24}C_1 + b_{25}C_2 + b_{26}C_1^2 + b_{27}C_2^2 + b_{28}C_1C_2)\sin v\tau\\
&\quad + \rho\lambda\chi_1(b_{29}\dot{C}_1 + b_{30}\dot{C}_2 + b_{31}C_1\dot{C}_1 + b_{32}C_1C_2 + b_{33}C_1\dot{C}_2 + b_{34}C_2\dot{C}_2\\
&\quad + b_{35}C_2\dot{C}_1)\cos v\tau + \rho\lambda\chi_0[(b_{36} + b_{37}C_1 + b_{38}C_2 + b_{39}C_1C_2)\dot{C}_1\\
&\quad + (b_{40} + b_{41}C_1 + b_{42}C_2 + b_{43}C_1C_2)\dot{C}_2 + \lambda^2(b_{44}\dot{C}_1^2 + b_{45}\dot{C}_1\dot{C}_2 + b_{46}\dot{C}_2^2\\
&\quad + b_{47}C_1\dot{C}_1^2 + b_{48}C_2\dot{C}_2^2 + b_{49}C_1\ddot{C}_1 + b_{50}C_2\ddot{C}_2 + b_{51}C_1^2\ddot{C}_1 + b_{52}C_2^2\ddot{C}_2) - \gamma\dot{C}_2
\end{aligned} \tag{29b}$$

where $a_i(X_1, X_2, \varphi_0)$, $b_i(X_1, X_2, \varphi_0)$ are rather cumbersome coefficients not presented here for brevity. Thus, we search for a solution of these equations in an expansion on the small parameter ε:

$$\begin{aligned}
C_1(\tau) &= C_{10}(T_0, T_1) + \varepsilon C_{11}(T_0, T_1),\\
C_2(\tau) &= C_{20}(T_0, T_1) + \varepsilon C_{21}(T_0, T_1).
\end{aligned} \tag{30}$$

After substitution of expressions (30) in system (29), we obtain an elementary eigenvalue problem to order ε^0:

$$\begin{aligned}
&a_1\frac{\partial^2 C_{10}}{\partial T_0^2} + a_3\frac{\partial C_{10}}{\partial T_0} + a_4\frac{\partial C_{20}}{\partial T_0} + a_5C_{10} = 0,\\
&b_2\frac{\partial^2 C_{20}}{\partial T_0^2} + b_3\frac{\partial C_{10}}{\partial T_0} + b_4\frac{\partial C_{20}}{\partial T_0} + b_6C_{20} = 0.
\end{aligned} \tag{31}$$

A solution for the problem to order ε^0 is taken as

$$\begin{aligned}
C_{10} &= A_1(T_1)\exp(\mathrm{i}\lambda_1 T_0) + \kappa_2 A_2(T_1)\exp(\mathrm{i}\lambda_2 T_0) + \text{c.c.},\\
C_{20} &= \kappa_1 A_1(T_1)\exp(\mathrm{i}\lambda_1 T_0) + A_2(T_1)\exp(\mathrm{i}\lambda_2 T_0) + \text{c.c.},
\end{aligned} \tag{32}$$

where c.c. is a complex conjugate of the first two terms in (32), κ_1, κ_2 are modal coefficients:

$$\kappa_j = -\frac{\mathrm{i}b_3\lambda_j}{b_2\lambda_j^2 + b_4 i\lambda_j - b_6} = -\frac{\mathrm{i}a_4\lambda_j}{a_1\lambda_j^2 + a_3 i\lambda_j - a_5}, \quad j = 1, 2. \tag{33}$$

The amplitudes A_1, A_2 of vibrations are treated now as functions of slow time variable. The problem to order ε^1 becomes (only the first equation is given here)

$$
\begin{aligned}
&a_1\frac{\partial^2 C_{11}}{\partial T_0^2}+a_3\frac{\partial C_{11}}{\partial T_0}+a_4\frac{\partial C_{21}}{\partial T_0}+a_5C_{11}=-2a_1\frac{\partial^2 C_{10}}{\partial T_0\partial T_1}-2a_2\frac{\partial^2 C_{20}}{\partial T_0\partial T_1}\\
&-a_3\frac{\partial C_{10}}{\partial T_1}-a_4\frac{\partial C_{20}}{\partial T_1}+a_7C_{10}^2+a_8C_{20}^2+a_9C_{10}C_{20}+a_{10}C_{10}^2C_{20}+a_{11}C_{10}C_{20}^2\\
&+a_{12}C_{10}^3+a_{13}C_{20}^3+\chi_1\rho\chi_0(a_{14}+a_{15}C_{10}+a_{16}C_{20})\cos\nu T_0\\
&+\nu\rho\lambda\chi_1(a_{23}+a_{24}C_{10}+a_{25}C_{20})\sin\nu T_0+\rho\lambda\chi_1\left(a_{29}\frac{\partial C_{10}}{\partial T_0}+a_{30}\frac{\partial C_{10}}{\partial T_0}\right)\cos\nu T_0\\
&+\rho\lambda\chi_0\left[(a_{36}+a_{37}C_{10}+a_{38}C_{20}+a_{39}C_{10}C_{20})\frac{\partial C_{10}}{\partial T_0}\right.\\
&\left.+(a_{40}+a_{41}C_{10}+a_{42}C_{20}+a_{43}C_{10}C_{20})\frac{\partial C_{10}}{\partial T_0}\right]-\gamma\frac{\partial C_{10}}{\partial T_0}.
\end{aligned}
\tag{34}
$$

The solution for the problem to order ε^1 can be expressed as follows:

$$
\begin{aligned}
C_{11}&=A_{111}(T_1)\exp(\mathrm{i}\lambda_1T_0)+A_{121}(T_1)\exp(\mathrm{i}\lambda_2T_0)+\text{c.c.},\\
C_{21}&=A_{112}(T_1)\exp(\mathrm{i}\lambda_1T_0)+A_{122}(T_1)\exp(\mathrm{i}\lambda_2T_0)+\text{c.c.}
\end{aligned}
\tag{35}
$$

To ensure a uniform validity of expansion (30), the following equations must have a trivial solution

$$
\begin{aligned}
&\eta_1A_{111}+\eta_2A_{112}=L_1,\\
&\eta_5A_{111}+\eta_6A_{112}=L_3.
\end{aligned}
\tag{36a}
$$

$$
\begin{aligned}
&\eta_3A_{121}+\eta_4A_{122}=L_2,\\
&\eta_7A_{121}+\eta_8A_{122}=L_4,
\end{aligned}
\tag{36b}
$$

where $\eta_1=-a_1\lambda_1^2+a_3\mathrm{i}\lambda_1+a_5$, $\eta_2=a_4\mathrm{i}\lambda_1$, $\eta_3=-a_1\lambda_2^2+a_3\mathrm{i}\lambda_2+a_5$, $\eta_4=a_4\mathrm{i}\lambda_1$, $\eta_5=-b_1\lambda_1^2+b_3\mathrm{i}\lambda_1+b_5$, $\eta_6=b_4\mathrm{i}\lambda_1$, $\eta_7=-b_1\lambda_2^2+b_3\mathrm{i}\lambda_2+b_5$, $\eta_8=b_4\mathrm{i}\lambda_1$; L_1, L_2, L_3, L_4 are presented in Appendix B.

As follows from the definition of the natural frequency, the principal determinants of both these systems vanish. Therefore, to cancel secular terms, both complementary determinants should also vanish. It is easy to show that if any one of them is zero along with the principal determinant, then the remaining one automatically equals zero. Thus, conditions of elimination of secular terms in asymptotic expansion (30) are formulated as

$$
\begin{aligned}
&\eta_1L_3-\eta_5L_1=0,\\
&\eta_3L_4-\eta_7L_2=0.
\end{aligned}
\tag{37}
$$

Straightforward algebraic manipulation results in a system of four amplitude modulation equations which are displayed here as

$$
\begin{aligned}
&\frac{\mathrm{d}c_1}{\mathrm{d}T_1}=f_1(c_1,c_2,\xi_1,\xi_2),\quad \frac{\mathrm{d}\xi_1}{\mathrm{d}T_1}=f_2(c_1,c_2,\xi_1,\xi_2),\\
&\frac{\mathrm{d}c_2}{\mathrm{d}T_1}=f_3(c_1,c_2,\xi_1,\xi_2),\quad \frac{\mathrm{d}\xi_2}{\mathrm{d}T_1}=f_4(c_1,c_2,\xi_1,\xi_2).
\end{aligned}
\tag{38}
$$

The explicit formulation of the functions f_i, $i=1,2,3,4$, is quite cumbersome. Here c_1, c_2, ξ_1, ξ_2 are amplitudes and phase angles of symmetric and skew-symmetric oscillations, $A_1=c_1(T_1)\exp(\mathrm{i}\xi_1(T_1))$, $A_2=c_2(T_1)\exp(\mathrm{i}\xi_2(T_1))$, see Eq. (32).

Some results of numerical analysis of resonant vibrations of a fluid-filled tube with the same parameters as given in Section 4.1, namely, $a=0.2$, $b=0.95$, $d=0.02$, $k=0.2$, $\rho=0.2$ and $\gamma=0.1$, are illustrated in Fig. 8, for three cases of loading by bending moments at $s_m=0.25$ and 0.75. Their magnitudes exceed the magnitude of moments considered in the previous part of the paper and each one of them makes condition (27) hold true. Curves 1 and 2 display the dependence of amplitudes of dominantly symmetric and dominantly skew-symmetric modes on the amplitude of flow pulsation for mean flow velocity of $\chi_0=0.1$ and curves 3 and 4 display the same dependence for $\chi_0=0.15$. Circles and rectangles denote amplitudes of vibrations obtained from direct numerical integration of 'modal' Eq. (29a) and (29b). Similar to the case treated in Section 4.1, for sufficiently small flow pulsation a zero solution is stable and no flexural vibrations develop. As pulsation amplitude reaches a certain threshold value (e.g., $\chi_1\approx0.0275$ for $\chi_0=0.1$, see Fig. 8(a)), the zero solution becomes unstable, whereas a single-mode nonlinear motion develops. However, this regime

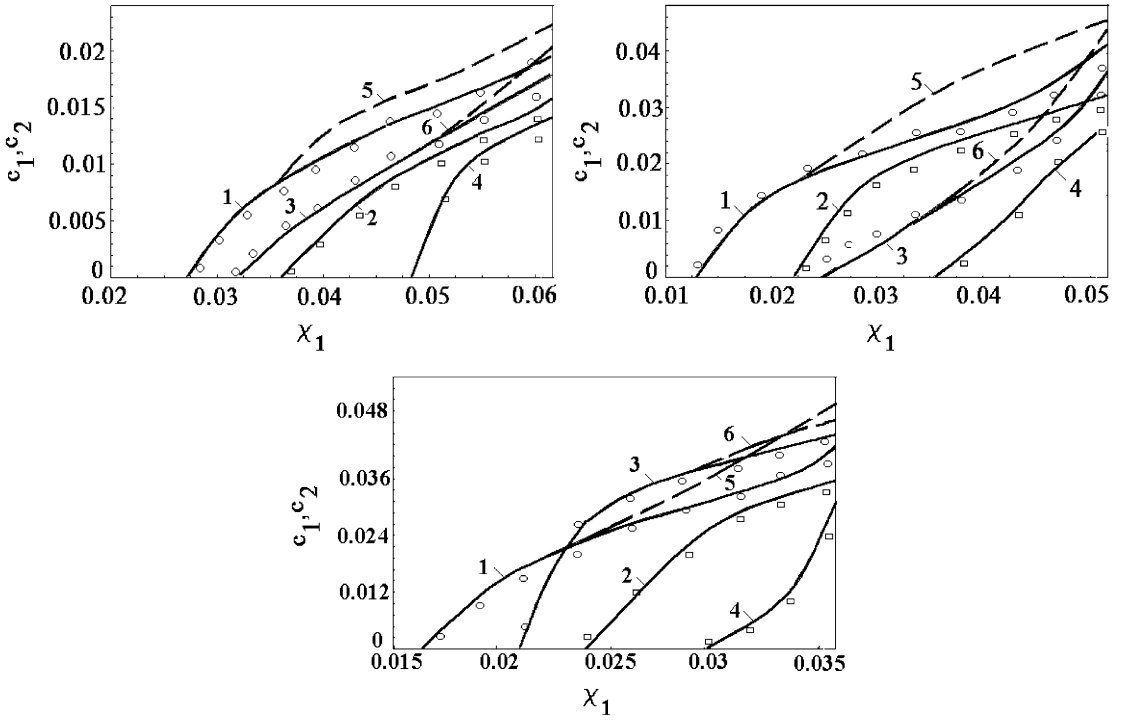

Fig. 8. (a) Amplitude response curves versus a magnitude of pulsating flow component for $M = 2.09 \times 10^{-4}$, (b). amplitude response curves versus a magnitude of pulsating flow component for $M = 1.19 \times 10^{-4}$ and (c) amplitude response curves versus a magnitude of pulsating flow component for $M = 2.99 \times 10^{-5}$.

of symmetric motions is stable in this particular case, only if $\chi_1 < 0.0354$. If the amplitude of flow pulsation exceeds this value, then a skew-symmetric component develops (curve 2) and the tube performs stable bi-modal vibrations. It should be pointed out that if the problem is solved in a single term approximation, then the dependence of the amplitude of symmetric motions is presented by the dashed curve 5, which smoothly emerges from curve 1 at $\chi_1 \approx 0.0354$ and lies well above its displayed part. Similarly, dashed curve 6 emerges from curve 3 for $\chi_0 = 0.15$, and the same holds true for all other cases illustrated in Fig. 8. Transition from a single modal to a bi-modal regime of motion is often characterised by a saturation phenomenon (Nayfeh, 1973; Thomsen, 1997), which manifests itself as 'locking' of the amplitude of a symmetric mode due to generation of a skew-symmetric component of motions and growth in its amplitude. In the case at hand, a single-mode solution is nonlinear and both amplitudes in the bi-modal regime remain dependent on the amplitude of pulsation. As is seen from Figs. 8(a–c), an increase in mean flow velocity stabilises the zero solution and pushes the occurrence of the bi-modal regime towards larger amplitudes of flow pulsation. In all three cases, the asymptotic results are fully confirmed by the direct numerical integration of Eqs. (29a) and (29b).

The case when bending moments are applied at the edges of a tube, i.e., at $s_m = 0.0$ and 1.0, has also been analysed. The magnitudes of bending moments have been chosen to produce the same static lateral deflections at $s = 0.5$ as in the previous case. Qualitatively, the amplitude response curve are much alike those in Figs. 8(a–c), and we do not display them here for brevity. Comparison of these two loading cases shows that much lower magnitudes of bending moments applied at $s_m = 0.0$ and 1.0 are required to produce the same maximum static lateral deflections. Also, the amplitudes of symmetric oscillations about initial static equilibrium position are always lower in the case of a fully curved tube than in the case of a tube curved only at the segment (0.25, 0.75).

5. Conclusions

A theoretical investigation of nonlinear static bending and vibrations of a simply supported nonuniform fluid-conveying tube is presented. The problem in statics of a tube with variable moment of inertia is solved numerically and

it is shown that for sufficiently slender tubes their behaviour is controlled by nonlinear geometry, whereas the contribution of nonlinear elasticity is very weak. Eigenfrequencies and eigenmodes of vibrations of a deformed tube are found in a solution of a linearised problem in dynamics. Analysis is restricted by the in-plane motions of a tube, i.e., motions developed in a plane of the initial static bending. It is shown that in the case of static bending by two symmetrically positioned moments, an internal parametric resonance is likely to occur between the first (symmetric) and the second (skew symmetric) modes. Then, the nonlinear dynamics of the deformed tube is addressed. The method of multiple scales is applied in the single and the bi-modal approximation to analyse the case of weak resonant excitation. Ranges of parameters of a flow pulsation which are related to a stable zero solution, a stable single-mode solution (when no internal parametric resonance occurs and also in the case of an internal parametric resonance) and a stable bi-modal solution (in the case of an internal parametric resonance) are found. The mean flow velocity component is shown to produce a stabilising effect. It is also shown that amplitudes of flow-induced vibrations are rather sensitive to static loading conditions.

Appendix A

The nonlinear coefficients in the single-mode approximation are as follows:

$$k_1 = \frac{\pi}{4}\lambda^2 \int_0^1 \left\{ \int_0^s (\alpha^2 - 1 + \rho) \int_0^s \varphi \cos\varphi_0 \, \mathrm{d}s^2 \cos\varphi_0 - \int_0^s (\alpha^2 - 1 + \rho) \int_0^s \varphi \sin\varphi_0 \, \mathrm{d}s^2 \sin\varphi_0 \right\} \varphi \, \mathrm{d}s,$$

$$k_2 = \int_0^1 \left\{ \beta_0 \cos\varphi_0 \varphi + \frac{\pi}{64}\bar{d}^2 [(\alpha^4 - 1)\varphi'' + 4\alpha^3 \alpha' \varphi'] - \frac{k\pi\bar{d}^4}{64} \Big[3(\alpha^6 - 1)(\varphi_0'^2 \varphi'' + 2\varphi_0' \varphi_0'' \varphi') + 18\alpha^5 \alpha' \varphi_0'^2 \varphi' \Big] - \frac{\pi}{4}\rho\chi_0^2 \cos 2\varphi_0 \varphi \right\} \varphi \, \mathrm{d}s,$$

$$k_3 = \int_0^1 \left\{ \frac{1}{2}\beta_0 \sin\varphi_0 \varphi^2 + \frac{k\pi\bar{d}^4}{64} \Big[3(\alpha^6 - 1)(2\varphi_0' \varphi' \varphi'' + \varphi_0'' \varphi'^2) + 18\alpha^5 \alpha' \varphi_0' \varphi'^2 \Big] - \frac{\pi}{4}\rho\chi_0^2 \sin 2\varphi_0 \varphi^2 \right\} \varphi \, \mathrm{d}s,$$

$$k_4 = \int_0^1 \left\{ \frac{1}{6}\beta_0 \cos\varphi_0 \varphi^3 + \frac{k\pi\bar{d}^4}{64} \Big[3(\alpha^6 - 1)\varphi'^2 \varphi'' + 6\alpha^5 \alpha' \varphi'^3 \Big] - \frac{\pi}{6}\rho\chi_0^2 \cos 2\varphi_0 \varphi^3 \right\} \varphi \, \mathrm{d}s,$$

$$k_8 = \frac{\pi}{4}\int_0^1 \varphi \sin 2\varphi_0 \, \mathrm{d}s, \quad k_9 = \frac{\pi}{2}\int_0^1 \varphi^2 \cos 2\varphi_0 \, \mathrm{d}s, \quad k_{10} = -\frac{\pi}{2}\int_0^1 \varphi^3 \sin 2\varphi_0 \, \mathrm{d}s,$$

$$k_{11} = \frac{\pi}{8}\int_0^1 \varphi \sin 2\varphi_0 \, \mathrm{d}s, \quad k_{12} = \frac{\pi}{4}\int_0^1 \varphi^2 \cos 2\varphi_0 \, \mathrm{d}s,$$

$$k_{13} = \frac{\pi}{4}\int_0^1 \left(\int_0^s \sin\varphi_0 \, \mathrm{d}s \cos\varphi_0 - \int_0^s \cos\varphi_0 \, \mathrm{d}s \sin\varphi_0 \right) \varphi \, \mathrm{d}s,$$

$$k_{14} = \frac{\pi}{4}\int_0^1 \left(\int_0^s \varphi \cos\varphi_0 \, \mathrm{d}s \cos\varphi_0 - \int_0^s \sin\varphi_0 \, \mathrm{d}s\varphi \sin\varphi_0 + \int_0^s \varphi \sin\varphi_0 \, \mathrm{d}s \sin\varphi_0 - \int_0^s \cos\varphi_0 \, \mathrm{d}s\varphi \cos\varphi_0 \right) \varphi \, \mathrm{d}s,$$

$$k_{15} = \frac{\pi}{8}\int_0^1 \left\{ -\int_0^s \sin\varphi_0 \, \mathrm{d}s\varphi^2 \cos\varphi_0 - \int_0^s \varphi \cos\varphi_0 \, \mathrm{d}s\varphi \sin\varphi_0 - \int_0^s \varphi^2 \sin\varphi_0 \, \mathrm{d}s \cos\varphi_0 + \int_0^s \cos\varphi_0 \, \mathrm{d}s\varphi^2 \sin\varphi_0 + \int_0^s \varphi si\varphi_0 \, \mathrm{d}s\varphi \cos\varphi_0 + \int_0^s \varphi^2 \cos\varphi_0 \, \mathrm{d}s \sin\varphi_0 \right\} \varphi \, \mathrm{d}s,$$

$$k_{16} = -\frac{\pi}{2}\int_0^1 \left(\int_0^s \varphi \cos\varphi_0 \, \mathrm{d}s \cos\varphi_0 + \int_0^s \varphi \sin\varphi_0 \, \mathrm{d}s \sin\varphi_0 \right) \varphi \, \mathrm{d}s,$$

$$k_{17} = -\frac{\pi}{2}\int_0^1 \left(-\int_0^s \varphi \cos\varphi_0 \, \mathrm{d}s\varphi \sin\varphi_0 - \int_0^s \varphi^2 \sin\varphi_0 \, \mathrm{d}s \cos\varphi_0 + \int_0^s \varphi \sin\varphi_0 \, \mathrm{d}s\varphi \cos\varphi_0 + \int_0^s \varphi^2 \cos\varphi_0 \, \mathrm{d}s \sin\varphi_0 \right) \varphi \, \mathrm{d}s,$$

$$k_{18} = -\frac{\pi}{2}\int_0^1 \left(\int_0^s \varphi\cos\varphi_0\,\mathrm{d}s\cos\varphi_0 + \int_0^s \varphi\sin\varphi_0\,\mathrm{d}s\sin\varphi_0\right)\varphi\,\mathrm{d}s,$$

$$k_{19} = -\frac{\pi}{2}\int_0^1 \left(-\int_0^s \varphi\cos\varphi_0\,\mathrm{d}s\varphi\sin\varphi_0 - \int_0^s \varphi^2\sin\varphi_0\,\mathrm{d}s\cos\varphi_0 + \int_0^s \varphi\sin\varphi_0\,\mathrm{d}s\varphi\cos\varphi_0 + \int_0^s \varphi^2\cos\varphi_0\,\mathrm{d}s\sin\varphi_0\right)\varphi\,\mathrm{d}s,$$

$$\begin{aligned} k_{20} = -\frac{\pi}{2}\int_0^1 \Bigg\{ &-\frac{1}{2}\int_0^s \varphi\cos\varphi_0\,\mathrm{d}s\varphi^2\cos\varphi_0 + \int_0^s \varphi^2\sin\varphi_0\,\mathrm{d}s\varphi\sin\varphi_0 - \frac{1}{2}\int_0^s \varphi^3\cos\varphi_0\,\mathrm{d}s\cos\varphi_0 \\ &- \frac{1}{2}\int_0^s \varphi\sin\varphi_0\,\mathrm{d}s\varphi^2\sin\varphi_0 + \int_0^s \varphi^2\cos\varphi_0\,\mathrm{d}s\varphi\cos\varphi_0 - \frac{1}{2}\int_0^s \varphi^3\sin\varphi_0\,\mathrm{d}s\sin\varphi_0\Bigg\}\varphi\,\mathrm{d}s, \end{aligned}$$

$$k_{21} = -\frac{\pi}{4}\int_0^1 \left(-\int_0^s (\alpha^2-1+\rho)\int_0^s \varphi^2\sin\varphi_0\,\mathrm{d}s^2\cos\varphi_0 - \int_0^s (\alpha^2-1+\rho)\int_s^1 \varphi^2\cos\varphi_0\,\mathrm{d}s\sin\varphi_0\right)\varphi\,\mathrm{d}s,$$

$$\begin{aligned} k_{22} = -\frac{\pi}{4}\int_0^1 \Bigg\{ &\int_0^s (\alpha^2-1+\rho)\int_0^s \varphi^2\sin\varphi_0\,\mathrm{d}s^2\varphi\sin\varphi_0 - \int_0^s (\alpha^2-1+\rho)\int_0^s \varphi^3\cos\varphi_0\,\mathrm{d}s^2\cos\varphi_0 \\ &- \int_0^s (\alpha^2-1+\rho)\int_s^1 \varphi^2\cos\varphi_0\,\mathrm{d}s^2\varphi\cos\varphi_0 + \int_0^s (\alpha^2-1+\rho)\int_s^1 \varphi^3\sin\varphi_0\,\mathrm{d}s^2\sin\varphi_0\Bigg\}\varphi\,\mathrm{d}s, \end{aligned}$$

$$\begin{aligned} k_{23} = -\frac{\pi}{4}\int_0^1 \Bigg\{ &-\int_0^s (\alpha^2-1+\rho)\int_0^s \varphi\cos\varphi_0\,\mathrm{d}s^2\varphi\sin\varphi_0 - \int_0^s (\alpha^2-1+\rho)\int_0^s \varphi^2\sin\varphi_0\,\mathrm{d}s^2\cos\varphi_0 \\ &- \int_0^s (\alpha^2-1+\rho)\int_s^1 \varphi\sin\varphi_0\,\mathrm{d}s^2\varphi\cos\varphi_0 - \int_0^s (\alpha^2-1+\rho)\int_s^1 \varphi^2\cos\varphi_0\,\mathrm{d}s^2\sin\varphi_0\Bigg\}\varphi\,\mathrm{d}s, \end{aligned}$$

$$\begin{aligned} k_{24} = -\frac{\pi}{4}\int_0^1 \Bigg\{ &-\frac{1}{2}\int_0^s (\alpha^2-1+\rho)\int_0^s \varphi\cos\varphi_0\,\mathrm{d}s^2\varphi^2\cos\varphi_0 + \int_0^s (\alpha^2-1+\rho)\int_0^s \varphi^2\sin\varphi_0\,\mathrm{d}s^2\varphi\sin\varphi_0 \\ &- \frac{1}{2}\int_0^s (\alpha^2-1+\rho)\int_0^s \varphi^3\cos\varphi_0\,\mathrm{d}s^2\cos\varphi_0 + \frac{1}{2}\int_0^s (\alpha^2-1+\rho)\int_s^1 \varphi\sin\varphi_0\,\mathrm{d}s^2\varphi^2\sin\varphi_0 \\ &- \int_0^s (\alpha^2-1+\rho)\int_s^1 \varphi^2\cos\varphi_0\,\mathrm{d}s^2\varphi\cos\varphi_0 + \frac{1}{2}\int_0^s (\alpha^2-1+\rho)\int_s^1 \varphi^3\sin\varphi_0\,\mathrm{d}s^2\sin\varphi_0\Bigg\}\varphi\,\mathrm{d}s. \end{aligned}$$

Appendix B

The left-hand sides of Eq. (36) are

$$\begin{aligned} L_1 = &-2\mathrm{i}a_1\lambda_1\frac{\mathrm{d}A_1}{\mathrm{d}T_1} - (a_3+\kappa_1 a_4)\frac{\mathrm{d}A_1}{\mathrm{d}T_1} + 2(a_7+\kappa_1 a_8)\bar{A}_1A_2\exp(\mathrm{i}\sigma_2T_0) \\ &+ a_9\kappa_1\bar{A}_1A_2\exp(\mathrm{i}\sigma_2T_0) + a_9\kappa_2\bar{A}_1A_2\exp(\mathrm{i}\sigma_2T_0) + 3a_{10}A_1^2\bar{A}_1\kappa_1 + 4a_{10}A_1A_2\bar{A}_2\kappa_2 \\ &+ a_{11}\kappa_1^2A_1^2\bar{A}_1 + 2a_{11}\kappa_1\kappa_2A_1A_2\bar{A}_2 + 2a_{11}\kappa_1^2A_1^2\bar{A}_1 + 2a_{11}\kappa_1\kappa_2A_1A_2\bar{A}_2 + 2a_{11}\kappa_2^2A_1A_2\bar{A}_2 \\ &+ 3a_{12}A_1^2\bar{A}_1 + 3a_{13}\kappa_1^3A_1^2\bar{A}_1 + \frac{\chi_1\rho\chi_0}{2}[a_{14}\exp(-\mathrm{i}\sigma_1T_0) + a_{15}A_2\exp(\mathrm{i}T_0(\sigma_1+\sigma_2)) \\ &+ a_{16}\kappa_2A_2\exp(\mathrm{i}T_0(\sigma_1+\sigma_2))] - \frac{\mathrm{i}\nu\lambda\chi_1}{2}[a_{23}\exp(-\mathrm{i}\sigma_1T_0) + a_{29}A_2\kappa_2\exp(\mathrm{i}T_0(\sigma_1+\sigma_2)) \\ &+ a_{30}\kappa_2\lambda_2A_2\exp(\mathrm{i}T_0(\sigma_1+\sigma_2))] + \frac{\mathrm{i}\rho\lambda\chi_1}{2}[a_{29}A_2\lambda_2\exp(\mathrm{i}T_0(\sigma_1+\sigma_2)) \\ &+ a_{30}\kappa_2\lambda_2A_2\exp(-\mathrm{i}T_0(\sigma_1+\sigma_2))] + \mathrm{i}\rho\kappa\chi_0\left[a_{36}\lambda_1A_1 + a_{37}(\bar{A}_1A_2\lambda_1\exp(\mathrm{i}\sigma_2T_0) + \bar{A}_1A_2\lambda_2\exp(\mathrm{i}\sigma_2T_0)\right] \\ &+ a_{38}(\bar{A}_1A_2\kappa_2\lambda_1\exp(\mathrm{i}\sigma_2T_0) + \bar{A}_1A_2\kappa_1\lambda_2\exp(\mathrm{i}\sigma_2T_0)) + a_{39}(A_1^2\bar{A}_1\kappa_1\lambda_1 + A_1A_2\bar{A}_2\kappa_1\lambda_1 \\ &+ 2A_1A_2\bar{A}_2\kappa_2\lambda_1 + A_1A_2\bar{A}_2\kappa_1\lambda_2 + 2A_1A_2\bar{A}_2\kappa_2\lambda_2) + a_{40}A_1\kappa_1\lambda_1 + a_{41}\bar{A}_1A_2\kappa_1\lambda_1\exp(\mathrm{i}\sigma_2T_0) \\ &+ a_{43}A_1^2\bar{A}_1\kappa_1^2\lambda_1 + 2a_{43}A_1A_2\bar{A}_2\kappa_1\kappa_2\lambda_1 + a_{42}\bar{A}_1A_2\kappa_1\kappa_2\lambda_1\exp(\mathrm{i}\sigma_2T_0) + a_{41}\bar{A}_1A_2\kappa_2\lambda_2\exp(\mathrm{i}\sigma_2T_0) \\ &+ 2a_{43}A_1A_2\bar{A}_2\kappa_2^2\lambda_2 + a_{42}\bar{A}_1A_2\kappa_1\kappa_2\lambda_2\exp(\mathrm{i}\sigma_2T_0) + a_{43}A_1A_2\bar{A}_2\kappa_1\kappa_2\lambda_2 + a_{43}\bar{A}_1A_2^2\kappa_2^2\lambda_2\exp(\mathrm{i}\sigma_2T_0) \\ &- \gamma\mathrm{i}\lambda_1A_1(1+\kappa_1); \end{aligned}$$

L_3 is similar to L_1 if the coefficients a_i are replaced by the coefficients b_i.

$$
\begin{aligned}
L_2 = & -2\mathrm{i}a_1\kappa_2\frac{dA_2}{dT_1} - a_3\frac{dA_2}{dT_1} + (a_7 + \kappa_1 a_8)A_1^2\exp(-\mathrm{i}\sigma_2 T_0) \\
& + a_9\lambda_1 A_1^2\exp(-\mathrm{i}\sigma_2 T_0) + a_{10}A_2^2\bar{A}_2\lambda_2 + 2a_{10}A_1A_2\bar{A}_1\lambda_2 \\
& + a_{11}\kappa_2^2A_2^2\bar{A}_2 + 2a_{11}\kappa_1^2A_1\bar{A}_1A_2 + 2a_{11}\kappa_1\kappa_2A_2A_1\bar{A}_1 + 2a_{11}\kappa_2^2A_2^2\bar{A}_2 + 3a_{12}A_2^2\bar{A}_2 \\
& + 3a_{13}\kappa_2^3A_2^2\bar{A}_2 + \frac{\chi_1\rho\chi_0}{2}[a_{15}A_1\exp(-\mathrm{i}T_0(\sigma_1+\sigma_2)) \\
& + a_{16}\kappa_1A_1\exp(-\mathrm{i}T_0(\sigma_1+\sigma_2))] - \frac{\mathrm{i}\nu\lambda\chi_1}{2}[a_{29}A_1\lambda_1\exp(-\mathrm{i}T_0(\sigma_1+\sigma_2)) \\
& + a_{30}\kappa_1\lambda_1A_1\exp(-\mathrm{i}T_0(\sigma_1+\sigma_2))] + \frac{\mathrm{i}\rho\lambda\chi_1}{2}[a_{29}A_1\lambda_1\exp(-\mathrm{i}T_0(\sigma_1+\sigma_2)) \\
& + a_{30}\kappa_1\lambda_1A_1\exp(-\mathrm{i}T_0(\sigma_1+\sigma_2))] + \mathrm{i}\rho\kappa\chi_0[a_{36}\lambda_2A_2 + a_{37}A_1^2\lambda_1\exp(-\mathrm{i}\sigma_2T_0) \\
& + a_{38}(A_1^2\kappa_1\lambda_1\exp(-\mathrm{i}\sigma_2T_0)) + a_{39}(3A_1A_2\bar{A}_1\kappa_1\lambda_1\exp(\mathrm{i}\sigma_2T_1) \\
& + 2A_1A_2\bar{A}_1\kappa_2\lambda_1\exp(\mathrm{i}\sigma_2T_1) + 2A_2^2\bar{A}_2\kappa_1\lambda_2 + A_1A_2\bar{A}_1\kappa_1\lambda_1 + 3A_2^2\bar{A}_2\kappa_2\lambda_2) + a_{41}A_1^2\kappa_1\lambda_1\exp(-\mathrm{i}\sigma_2T_0) \\
& + a_{42}A_1^2\kappa_1^2\lambda_1\exp(-\mathrm{i}\sigma_2T_1) + a_{43}A_1A_2\bar{A}_2\kappa_1^2\lambda_1 + 3a_{43}\bar{A}_1A_1A_2\kappa_1^2\lambda_1 + 2a_{43}A_1A_2\bar{A}_1\kappa_1\kappa_2\lambda_1 \\
& + 3a_{43}A_2^2\bar{A}_2\kappa_2^2\lambda_2 + a_{40}A_2\kappa_2\lambda_2 + a_{43}A_1A_2\bar{A}_1\kappa_1\kappa_2\lambda_2 + 2a_{43}\bar{A}_2A_2^2\kappa_1\kappa_2\lambda_2 \\
& - \gamma\mathrm{i}\lambda_2A_2(1+\kappa_2);
\end{aligned}
$$

L_4 is similar to L_2 if the coefficients a_i are replaced by the coefficients b_i.

References

Banichuk, N.V., Tchernousko, F.L., 1973. Variational Problems in Mechanics and Control Theory. Nauka, Moscow (in Russian).

Langthjem, M.A., Sugiyama, Y., 2000. Dynamic stability of columns subjected to follower loads: a survey. Journal of Sound and Vibration 238, 809–851.

Nayfeh, A.H., 1973. Perturbation Methods. Wiley, New York.

Paidoussis, M.P., 1998. Fluid–Structure Interaction. Slender Structures and Axial Flow, Vol. 1. Academic Press, London.

Semler, C., LI, G.X., Paidoussis, M.P., 1994. The nonlinear equations of motion of pipes conveying fluid. Journal of Sound and Vibration 169, 577–599.

Svetlitskij, V.A., 1987. Mechanics of Rods, Part 2: Dynamics. Vysshaja Shkola, Moscow (in Russian).

Tchernykh, K.F., 1978. Nonlinear Elasticity. Leningrad University Press, Leningrad (in Russian).

Thomsen, J.J., 1997. Vibrations and Stability. Order and Chaos. McGraw-Hill, London.

Timoshenko, S.P., 1936. Theory of Elastic Stability. McGraw-Hill, New York.

Wolfram, S., 1991. Mathematica: A System for Doing Mathematics by Computer. Addison-Wesley, Reading, MA.